

Nonuniform Spatial Sampling in a Ground-Based Noise SAR

Łukasz Maślikowski and Jacek Misiurewicz

Abstract—The paper presents an idea of nonuniform spatial sampling applied to a noise synthetic aperture radar. In certain cases it is desirable to limit the number of spatial (along-track) domain samples acquired in a SAR radar because of external constraints on sampling frequency or on the overall number of samples – e.g. in order to economy on time or power consumed. Lowering number of samples taken may, however, lead to spatial aliasing and incorrect reconstruction of the image. Nonuniform sampling allows to reduce the aliasing effect and reconstruct the image better. This technique can be applied with standard reconstruction methods, but it works best together with Compressive Sensing reconstruction algorithms. The idea will be verified with an experimental noise SAR built at ISE PW.

Keywords—Nonuniform sampling, noise radar, synthetic aperture radar (SAR), compressive sampling.

I. INTRODUCTION

NOISE radar technology is gaining popularity nowadays [1], [2]. Allowing to use very long integration time, it permits to use low transmitted power. However, in the SAR application it makes the overall measurement time very long, as a sufficient number of spatial samples has to be taken to cover the required baseline without compromising the spatial unambiguity.

With traditional approach, the spatial unambiguity is reached by setting the radar antenna positions spaced according to the Nyquist criterion for the Doppler frequency induced by antenna movement. For the worst case (an object located in the track direction), this criterion reduces to $1/4$ wavelength spacing of the spatial samples (or antenna positions with the stop-and-go image acquisition).

In the experimental noise radar system designed and built at Institute of Electronic Systems, Warsaw University of Technology (ISE PW) [3], [4], the above requirement, together with the stepped-frequency method of wideband waveform synthesis [5] results in barely acceptable total acquisition times. Similar problem may exist in a stratospheric UAV or a pico-satellite environment, where the limiting factor for the number of acquired samples may be imposed by severe limitation on the available power and energy (the power is usually gained from solar panels during weeks-long flight). In these cases, if the main processing is done in the ground segment, also the on-board storage capacity or speed of the down-link for transmission of raw data from the vehicle to the Earth may impose such a limit.

This work was supported by the Polish Ministry of Science and Higher Education under Commissioned Research Project PBZ-MNiSW-DBO-04/I/2007.

Łukasz Maślikowski and Jacek Misiurewicz are with the Institute of Electronic Systems, Warsaw University of Technology, Nowowiejska 15/19, 00-665 Warsaw, Poland (e-mails: L.Maslikowski@stud.elka.pw.edu.pl, jmisiure@elka.pw.edu.pl).

The traditional (Nyquist) limitation may be, however, lifted if some additional information on the signal model is known. Such an approach forms the base of compressive sampling theory [6], where nonuniform sampling is used to gather enough information on a signal to be able to reconstruct it. Good results are obtained if the signal model is *sparse*, which translates into the model of the radar scene composed of limited number of bright points.

Similar approach – with assumption of a simple signal model – was also used for exceeding the Nyquist limit in Doppler frequency estimation in MTI radar [7]–[9]. Nowadays the sparse signal approach is being investigated with respect to SAR radars [10]–[13].

In a SAR radar, the sampled Doppler signal is only an intermediate step in construction of radar image. Thus, after sub-Nyquist sampling the original signal need not be reconstructed, if other way of proceeding towards an image is available. Such a way is provided by the compressive sampling theory, where the representation of a signal in a chosen parameter space is sought with ℓ_1 -norm minimization technique.

The compressive sampling theory also indicates the effective distribution of samples – one of the most intuitive results is that random selection of sampling points is usually a good choice.

With an assumption of signal model composed of several point-like scatterer echoes at each range resolution bin, the calculations show that a number of sampling points along the baseline may be reduced several times with respect to the Nyquist sampling.

In the following, the reconstruction problems will be studied with respect to the (already mentioned) ground based experimental SAR system working with noise radar technology. The system, built at Warsaw University of Technology (ISE PW), consists of rail-mounted antenna carriage (shown in Fig. 1) and a set of RF and signal processing equipment. The rail length, or the synthetic aperture size, is limited by the available terrace length. With poor antenna directivity, the imaged scene may be much wider than the aperture size. This adds to the geometrical complexity, especially with the range migration correction.

II. SAR IMAGE RECONSTRUCTION

SAR imaging is performed with a radar platform moving perpendicularly to the imaging direction. Thus, objects in the field of view modulate the reflected wave due to Doppler effect, as their distance to the radar first diminishes, then starts to increase. This modulation is present in the received baseband signal as a complex chirp.



Fig. 1. SAR antennas at ISE PW “terrace SAR” lab.

In a SAR image reconstruction, it is assumed that a baseband signal received from one range cell is composed from chirps generated by each of the reflecting points in the investigated range throughout the antenna beamwidth. During signal processing, the received signal is analyzed to find the location (and echo amplitude) of reflectors comprising the scene.

The signal from one range cell is naturally sampled in the cross-range dimension because of range processing which is performed in the block mode. In stop-and-go systems, such as the one built at ISE PW, the spatial (cross-range) sampling is additionally forced by the principle of operation.

Maximum frequency present in the baseband received signal determines the minimum sampling rate that is acceptable (based on traditional approach). It is straightforward to see that the maximum spatial frequency can be described as

$$k_{max} = 2v \sin \alpha / \lambda \quad (1)$$

where v is the radar platform velocity, and α is the half-width of the antenna beam.

The problem that will be investigated in the following, can be stated as a question if the image can be properly reconstructed with lower spatial sampling rate than $2 \cdot k_{max}$ as imposed by the sampling theorem.

III. COMPRESSIVE SAMPLING APPLICATION TO SAR

Compressive sampling theory (also known as compressed sensing or CS) has been developed in recent years [6], [14]–[16]. The main assertion of this theory is that one can recover many kinds of signals from fewer samples than the traditional approach requires. This relies on the *sparsity* property of the signal, i.e. the possibility to express the signal as a linear combination of a small subset of vectors belonging to a chosen basis.

In the mathematical formulation of CS theory [6], it is assumed that a signal $s(t)$ can be represented in a basis

$$\Psi = [\psi_1 \psi_2 \dots \psi_M]$$

$$s(t) = \sum_{m=1}^M x_m \psi_m \quad (2)$$

where x is a coefficient sequence that (in a case of orthonormal basis) may be computed as $x_m = \langle f, \psi_m \rangle$.

The traditional sampling theory requires M measurements (samples) of the signal $s(t)$ in order to reconstruct it (without imposing any additional constraints). The CS theory states that an exact reconstruction of a signal is possible with much smaller number of samples, if the signal is known to have all but S out of M coefficients x_m equal to zero, where $S \ll M$ (S defines *sparsity* of the signal). The choice of samples defines a *sensing basis* Φ , and the coherence $\mu(\Phi, \Psi)$ between bases affects the number of necessary samples. If the signal belongs to R^n space, the coherence is calculated as

$$\mu(\Phi, \Psi) = \sqrt{n} \cdot \max_{1 \leq k, j \leq n} |\langle \phi_k, \psi_j \rangle| \quad (3)$$

A theorem cited in [6] states that the reconstruction of the coefficient sequence as the minimal ℓ_1 norm one that is consistent with the measured data is exact with high probability, if the number of measurements m satisfies the condition

$$m \geq C \cdot \mu^2(\Phi, \Psi) \cdot S \cdot \log n \quad (4)$$

for some positive constant C and the measurements are chosen from the basis Φ uniformly at random. The value of C depends on the signal class and on the desired probability level. As seen in [6], for typical problems the value is not very high.

In a SAR application the signal basis Φ would be comprised of shifted chirp signals, so the sequence of coefficients x corresponds to the amplitudes of elementary reflector echoes. The sparsity condition is therefore equal to the model of the SAR scene as composed of a limited number of bright points.

Minimum- ℓ_1 norm solution corresponds in this case to a solution with minimum sum of RCS's of the reflectors.

The sensing basis Φ in the case of SAR radar may be composed of a series of $\delta(l - l_i)$ unit sample functions located at the uniform spatial sampling locations l_i satisfying Nyquist criterion. Then, m of these locations are selected for measuring the signal.

With a simple SAR analysis, a narrow antenna pattern is assumed. In consequence, the range to the reflecting object $r(t)$ is approximated to be changing in the quadratic manner, resulting in a linear frequency modulation (chirp) pattern of a reflected signal. This approach will be used below to demonstrate the applicability of CS to the SAR detection.

In the wide antenna pattern case, as with the ISE PW “terrace SAR” experiment, two additional complications have to be taken into account. First, higher order terms in the $r(t)$ dependency cannot be neglected. Thus, the chirp pattern is not linear any more. Second, the $r(t)$ distance changes significantly – the change may well exceed the range resolution cell size. In consequence, the detection process must include range cell migration compensation, which is an operation performed in the slant-range dimension. This approach will be used below with the second series of simulations.

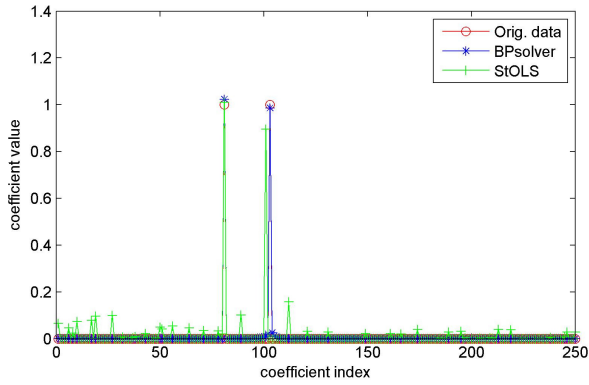


Fig. 2. Multi-chirp signal coefficients x_i recovered by CS methods.

IV. SIMULATION RESULTS

A simulation has been performed in order to demonstrate the applicability of CS idea to the detection of chirps in a signal.

A basis Ψ has been formed as a Matlab matrix consisting of 1000 shifted chirp signals. A signal $s(t)$ was composed of $S = 2$ randomly chosen base vectors. Small number $m = 50$ samples of s were calculated at randomly chosen locations and the problem of reconstruction (i.e. finding coefficients x_i representing the signal s in basis Ψ) was solved using two methods from sparse toolboxes presented in [17] and [18].

Example results are shown at Fig. 2, where the recovered coefficients are shown against the original ones. Results labelled “BP solver” refer to the ℓ_1 method from [17] and “StOLS” refers to the Stagewise Orthogonal Least Squares from [18]. The latter performed satisfactorily in other experiments, though with this application the former outperforms it – the ℓ_1 method reconstructs much cleaner image.

Another simulation experiment has been conducted to show the possibility of sub-Nyquist sampling of SAR signal. The received signal with a single reflector in field of view has been generated and processed with traditional (matched filtering) methods. A simulator framework developed for the “terrace SAR” has been employed. The target has been placed at 40 m from the aperture. Other simulation parameters were as follows:

- Imaged scene: 80x80 m
- Carrier frequency: 2 GHz
- Sounding signal bandwidth: 36 MHz
- Antenna 3dB mainlobe width: 170°

The signal processing for the SAR image reconstruction consists of the following steps [3].

- The received signal at each antenna position is correlated with a copy of the transmitted signal to obtain a *range profile*. This stage is called *range compression* and is mathematically equivalent to matched filtering.
- For each pixel of reconstructed image, samples from relevant range cells, corresponding to $r(t)$ changing with antenna position, are collected in a vector (range cell migration correction).

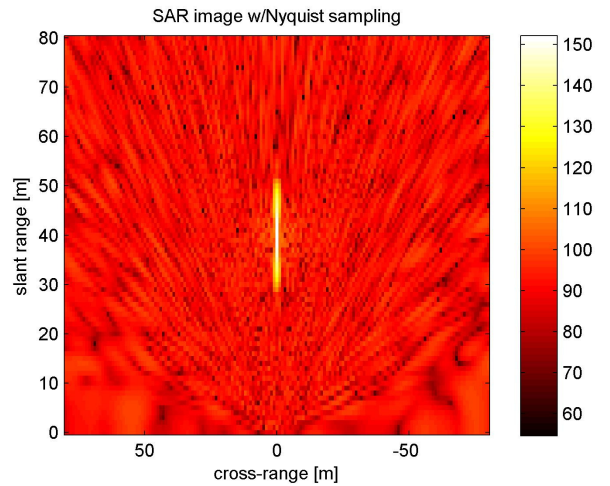


Fig. 3. Whole SAR picture recovered with Nyquist sampling.

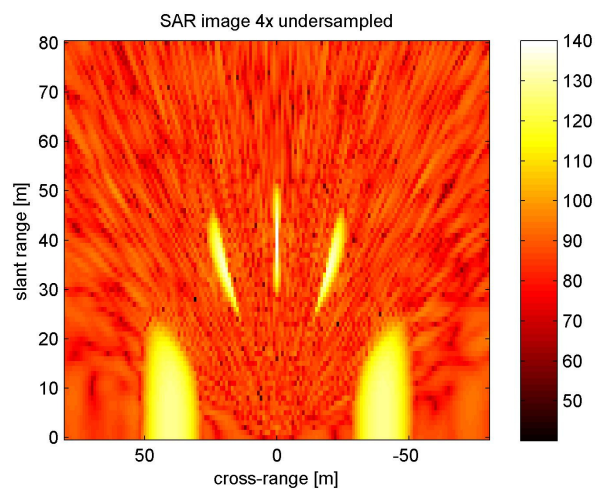


Fig. 4. Whole SAR picture with 4x undersampling (uniform).

- For each pixel a matched filter in the cross-range direction is designed.
- The amplitude of signal at the pixel is calculated as the result of correlating the range-corrected received signal with the matched filter template.

In the first experiment within the series, a reference picture has been reconstructed with Nyquist sampling (Fig. 3).

Next, the same picture has been reconstructed from the samples decimated uniformly by a factor of 4. Sub-Nyquist sampling artefacts are clearly visible (Fig. 4) in the form of spurious detections on a circle defined by the position of a real target.

Finally, the picture has been again reconstructed from the same number of samples (equal to 1/4 of number of Nyquist samples), but this time samples were taken in a nonuniform (staggered) manner. The staggering was done by randomly choosing the inter-sample periods from a set of predefined periods not being a multiple of the Nyquist period (Fig. 5). Sub-Nyquist sampling artefacts are still visible, however they are not so sharp and not so prominent as in the previous example.

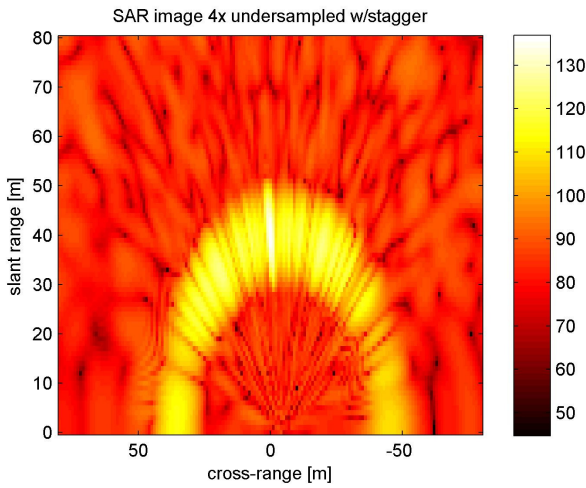


Fig. 5. Whole SAR picture with 4x undersampling (staggered).

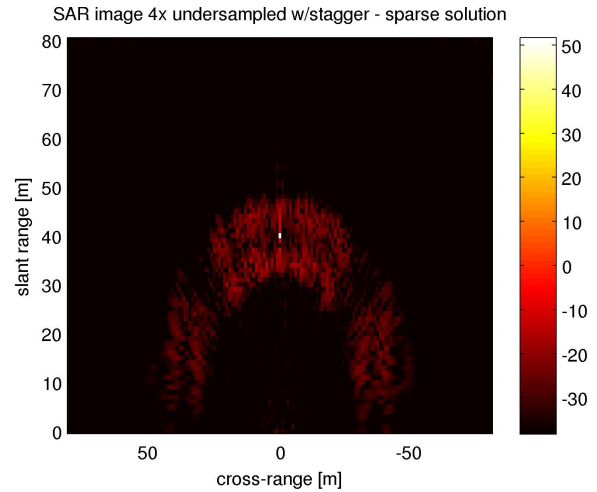


Fig. 8. Simulation results for CS method.

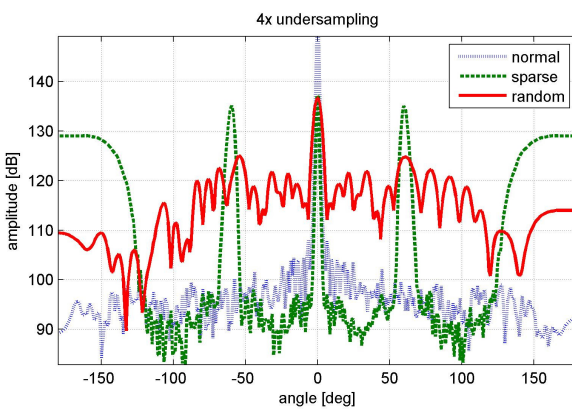


Fig. 6. Simulation results for 4x undersampling.

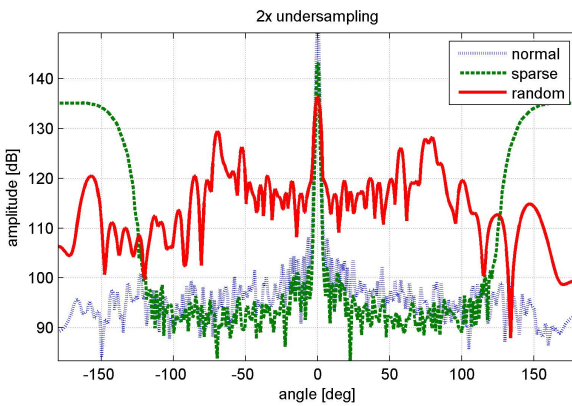


Fig. 7. Simulation results for 2x undersampling.

Finally, at Fig. 6 cross-sections of the above pictures along the half-circle line comprising the maxima of the reconstructed image are shown. The comparison shows that the staggered choice of sampling instants allow to make the artifacts less visible, although the reduction in the number of sampling points is not without penalty on the image contrast.

Similar diagram for the case of undersampling by a factor of 2 is shown at Fig. 7.

It must be underlined that in the above experiments a CS method was not used. Instead, a traditional matched filter method was used, employing well-known efficient algorithms. The results from the previous experiment indicated that CS methods can be expected to improve much on the image quality.

In order to confirm this opinion, a CS experiment has been performed. The same simulation setup with staggered undersampling was used. It must be however noted that the processing in this case differs significantly from the standard (matched filtering) approach.

In the matched filter approach with range migration in effect, each pixel of the image has to be reconstructed separately – the correction of range migration is different for each pixel. With this separation, the final correlation step is performed on one-dimensional vectors which simplifies the processing.

The CS approach requires construction of a signal basis Ψ which – taking into respect range migration – consists of two-dimensional signals, spanning cross-range due to antenna movement and slant-range due to the migration. In the result, the basis Ψ has the number of elements equal to the number of analyzed pixels, where each element consists of signal template samples from the whole cross- and slant- range domain.

In the described experiment, the image was computed with 1 m resolution, so the basis was composed of $81 \cdot 81 = 6561$ elements. Each element was a $75 \cdot 39 = 2925$ samples range profile template matrix.

The image reconstruction process consisted of the following steps.

- Calculating undersampled set of range profiles (same as with standard processing).
- Preparing the basis with (undersampled) range profile templates for all the pixels.
- Using the iterative ℓ_1 solver from the toolbox [17] to find a best CS solution.

In the result, an image shown in Fig. 8 has been obtained. First, exceptional dynamic range of the Fig. 8 image with respect to traditional reconstruction has to be noted. Second,

the CS method resulted in reconstructing an image with just *one* bright pixel. This is an effect of the *signal sparsity* assumption inherent in the CS approach – the CS method will always prefer a solution minimizing number of prominent x_m coefficients (in this application – bright pixels in the reconstructed image).

V. PRACTICAL APPLICATION REMARKS

In a practical application a limiting factor may be nowadays the data processing. Known ℓ_1 minimization algorithms, as opposed to least squares minimization, require iterative approach which induces high numerical complexity and non-deterministic run times. The available processing power is, however, still increasing with use of parallel computations and specialized processors. Also, new fast algorithms are being developed by the CS community. A good example of algorithms that may be employed for speedup of processing may be found in [19].

VI. CONCLUSION

The results presented here came from a need to optimize sampling for a noise SAR radar. They are, however, applicable also to other SAR radars as well.

The compressive sensing methods solve the image reconstruction problem in SAR radar exceptionally well. It must be however noted that CS solution is based on the sparse signal model. In the result, the application of CS method must be preceded by a study of the scene sparsity. Some cases of inherently sparse scene have been investigated in the literature – e.g. GMTI scene in [12] or a special case of ground-and-building bounce in [13].

An experiment confirming the effectiveness of the described idea is under development. It will be performed using the SAR noise radar system designed and built at Warsaw University of Technology.

REFERENCES

- [1] K. Kulpa, K. Lukin, W. Miceli, and T. Thayaparan, "Editorial: Signal Processing in Noise Radar Technology," *IET Radar, Sonar & Navigation*, vol. 2, no. 4, pp. 229–232, 2008.
- [2] K. Kulpa, K. Lukin, J. Misiurewicz, Z. Gajo, A. Mogila, and P. Vyplavin, "Quality Enhancement of Image Generated with Bistatic Ground Based Noise Waveform SAR," *IET Radar, Sonar & Navigation*, vol. 2, no. 4, pp. 263–273, 2008.
- [3] Ł. Maślowski, M. Malanowski, K. S. Kulpa, and C. Contartese, "Preliminary Results of Ground-Based Noise SAR Experiments," in *8th European Conference on Synthetic Aperture Radar (EuSAR)*. Aachen, Germany: VDE Publishing House, 2010, pp. 596–599.
- [4] Ł. Maślowski and K. Kulpa, "Bistatic Quasi-Passive Noise SAR Experiment," in *11th International Radar Symposium (IRS)*, June 2010, pp. 1–3.
- [5] Ł. Maślowski and M. Malanowski, "Sub-Band Phase Calibration in Stepped Frequency GB Noise SAR," in *European Radar Conference (EuRAD)*, October 2010, pp. 200–203.
- [6] E. Candes and M. Wakin, "An Introduction to Compressive Sampling," *Signal Processing Magazine*, vol. 25, no. 2, pp. 21–30, March 2008.
- [7] J. Misiurewicz, "Unambiguous Doppler Frequency Estimation in an MTI Radar," in *Proceedings of International RADAR 97 Conference*, Edinburgh, Scotland, 1997, pp. 530–534.
- [8] L. T. Younkins, "Velocity Estimation for Radar Systems with Staggered Pulse Repetition Frequency," in *Proceedings of International RADAR 97 Conference*, Edinburgh, Scotland, 1997, pp. 425–428.
- [9] C. Lemke, T. Mahr, and H.-G. Kölle, "Coherent Parameter Estimation for Radar Signals," in *Proceedings of International Radar Symposium*, Cologne, Germany, 2007, pp. 145–150.
- [10] D. Li, Y. Hou, and W. Hong, "The Sparse Array Aperture Synthesis with Space Constraint," in *8th European Conference on Synthetic Aperture Radar (EuSAR)*. Aachen, Germany: VDE Publishing House, 2010, pp. 950–953.
- [11] B. Zhang, H. Jiang, W. Hong, and Y. Wu, "Synthetic Aperture Radar Imaging of Sparse Compressed Sensing," in *8th European Conference on Synthetic Aperture Radar (EuSAR)*. Aachen, Germany: VDE Publishing House, 2010, pp. 689–692.
- [12] L. Prünke, "Application of Compressed Sensing to SAR/GMTI-Data," in *8th European Conference on Synthetic Aperture Radar (EuSAR)*. Aachen, Germany: VDE Publishing House, 2010, pp. 465–469.
- [13] X. Zhu and R. Bamler, "Super-Resolution for 4-D SAR Tomography via Compressive Sensing," in *8th European Conference on Synthetic Aperture Radar (EuSAR)*. Aachen, Germany: VDE Publishing House, 2010, pp. 273–276.
- [14] E. Candes and T. Tao, "Near-Optimal Signal Recovery from Random Projections: Universal Encoding Strategies?" *IEEE Transactions on Information Theory*, vol. 52, no. 12, pp. 5406–5425, December 2006.
- [15] E. Candes, J. Romberg, and T. Tao, "Robust Uncertainty Principles: Exact Signal Reconstruction from Highly Incomplete Frequency Information," *IEEE Transactions on Information Theory*, vol. 52, no. 2, pp. 489–509, February 2006.
- [16] D. Donoho, "Compressed Sensing," *IEEE Transactions on Information Theory*, vol. 52, no. 4, pp. 1289–1306, April 2006.
- [17] G. Peyre, "Toolbox Sparsity – Sparsity-Based Signal Processing Related Functions," 12 April 2010.
- [18] A. Majumdar, "Orthogonal Least Squares Algorithms for Sparse Signal Reconstruction," 12 April 2010.
- [19] W. Yin, S. Morgan, J. Yang, and Z. Yin, "Practical Compressive Sensing with Toeplitz and Circulant Matrices," 12 April 2010.